Study on the Influence of Eccentricity on Oil Film Instability of Rotor System

Yuegang Luo[1,2], Hao Xu[1,2],Hao Fu[1,2],Pengfei Wang[1,2],Chenyong Wang[1,2]
1.College of Mechanical and Electronic Engineering, Dalian Minzu University
2.State Key Laboratory of Intelligent Perception and Advanced Control of State Ethnic Affairs Commission, Dalian Minzu University
Dalian China
luoyg@dlnu.edu.cn; 528235288@qq.com; 1742971914@qq.com; 2861014893@qq.com; 932332150@qq.com;

***Abstract*—Oil film oscillation is one of the most important faults in rotating machinery. It is important to find out the fault characteristics of oil film instability and make early diagnoses. Numerical simulation and test were carried out on the double-span rotor test-bed so as to simulate the oil film instability of the actual machine. In the numerical calculation, the dynamic model of the test-bed was established by using Zhang Wen unsteady non-linear bearing oil film force model, which is based on the finite element method. Effects of different eccentricities on the system response were compared and analyzed. The influence of different eccentricity on the dynamic response of the system was analyzed by test. The results show that oil film instability can induce higher amplitude oil film oscillation frequency. The low frequency components caused by oil film instability dominate in the high speed region. Alone with increasing eccentricity, the amplitude of oil film oscillation frequency decreases. It restrains the influence of oil film oscillation on system operation to a certain extent. The fault characteristics provide a practical basis for identifying oil film instability in the future.**

Keywords-component; Rotating machinery; Oil film instability; Experiments; Dynamic characteristics

I. INTRODUCTION

Modern rotating machinery is developed towards high speed, high power and high load. Sudden accidents are more frequent than before and has caused huge economic losses. Rotor is the core component of rotating machinery. Oil film instability is a kind of frequent failure of high-speed and light-load flexible rotor. At present, domestic and foreign scholars primarily focus on numerical simulation analysis and experimental research, and have achieved abundant results.

For simulating the nonlinearity of the sliding bearing better, some nonlinear oil-film force models have been established, such as in literatures [1,2]. Xiang et al. [3] established the model of asymmetric double rotor-bearing system. The interaction between collision friction and oil film force is studied. The numerical results show that the performance of the nonlinear dynamic system varies with the change of rotational speed and model parameters. The nonlinear dynamic behaviors of a rotor-bearing system is studied by Jing et al [4,5], considering the oil whip phenomenon. Ma et al. [6,7] analyzed the dynamic characteristics of the rotor-bearing system used by Capone oil film force model. Ma et al. [8] established a twin-rotor system with gyroscopic effect and adopted a lumped mass model. The eccentricity and anti-phase conditions of two rotating discs are studied. The dynamic characteristics of the system are reflected by the response diagram during the speed-up process. In references [9,10], the system with rotor's oil fluid instability question was studied on a test rig.

Because the literatures mostly concentrate on the analysis of single-span rotor system, the complex dynamic behavior of oil hydraulic instability faults in multi-span system is seldom studied. A two-span rotor model supported by sliding bearings is established. Based on the finite element theory, the oil film instability faults of double-span rotor-bearing system are numerically calculated by using Zhang Wen's unsteady non-linear oil hydraulic force model [2], and draws a conclusion that the oil film instability faults of double-span. At the same working condition, the axle center trajectory, time domain waveform, spectrum and Poincare cross-section are compared and analyzed. At the same time, the test bench is used to test, and the vibration signals of bearings under different eccentricities and rotational speeds are compared and analyzed by using three-dimensional waterfall diagram, axle center trajectory and spectrum diagram, so as to analyze the fault characteristics of oil film instability and provide a certain theoretical and practical basis for identifying system faults in the future.

II. MODEL OF DOUBLE-SPAN ROTOR SYSTEM

A. Model of Rotor System

The dual-span system with rotors and bearings model is

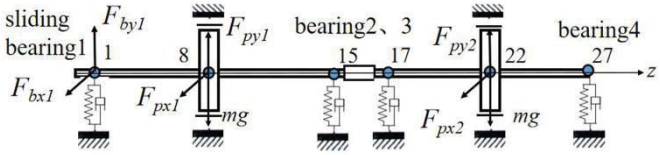

Figure 1. Two-span Rotor-Bearing System Model

Funding projects: National Natural Science Foundation of China (No. 51875085) and Liaoning Natural Science Foundation (No. 20170540205, 20180551073)

978-1-7281-0860-5/19/$31.00 ©2019 IEEE

shown in Figure 1. The model is discretized into 26 axle segments (27 nodes) by finite element method. The weight of the left and right discs is 800g. The mass of the discs is concentrated on the nodes 8 and 22. The bearings of nodes 1, 15, 17 and 27 are simplified as spring dampers. The axis segment is imitated by Timoshenko beam element. The double section drops *A* and *B* of the beam element have six degrees of freedom. The displacement and revolving angles of drop *A (B)* in *x*, *y* and *z* directions are *xA(xB)* 、 *yA(yB)* 、 *zA(zB)* and *θxA(θxB)* 、 *θyA(θyB)* 、 *θzA(θzB)* respectively. Because the axial deformation of the actual system is smaller than that of bending and torsion, the shift and revolving angles of node *A (B)* in *x*, *y* and *z* directions are neglected. The generalized coordinates of the displacement between two endpoints can be expressed as:

$$\boldsymbol{u}=[x_A,y_A,\theta_{xA},\theta_{yA},x_B,y_B,\theta_{xB},\theta_{yB}]^{\mathrm{T}} \tag{1}$$

The equation of the whole system is:

$$\boldsymbol{M}\ddot{\boldsymbol{u}}+(\boldsymbol{C}+\boldsymbol{D})\dot{\boldsymbol{u}}+\boldsymbol{K}\boldsymbol{u}=\boldsymbol{Q} \tag{2}$$

Among them, $\boldsymbol{M}$ is the system's mass matrix, $\boldsymbol{C}$ is the damping matrix, $\boldsymbol{D}$ is the gyro matrix, $\boldsymbol{K}$ is the stiffness matrix, $\boldsymbol{Q}$ is the combined external force vector. The same:

$$\boldsymbol{Q}=\boldsymbol{F_b}+\boldsymbol{F_p}+\boldsymbol{G} \tag{3}$$

In the formula, $\boldsymbol{F_b}$ is the oil force vector of the system, $\boldsymbol{F_p}$ is eccentric force vector and $\boldsymbol{G}$ is gravity vector.

B. *Zhang Wen Non-steady State Nonlinear Oil Film Force Model*

Zhang Wen non-linear unsteady oil film force model [2] is used. The formulas are as follows:

$$F_b=\sigma\times f_b \tag{4}$$

$$\sigma=\eta\omega\frac{D}{2}L\left(\frac{D}{2\delta}\right)^2\left(\frac{L}{D}\right)^2 \tag{5}$$

In the formula, σ is Sommerfeld number. η is the viscosity of lubricating oil and δ is the clearance of oil film, which can be found in the mechanical design manual. *L* is the width of the bearing, *D* is the diameter of bearing, ω is journal rotation angular velocity, and f_b is the dimensionless form of the oil force. Its component along the *x* and *y* directions is expressed as follows:

$$\begin{Bmatrix} f_{bx} \\ f_{by} \end{Bmatrix} = -\begin{pmatrix} C_{11} & C_{12} \\ C_{21} & C_{22} \end{pmatrix}\begin{pmatrix} \dot{X} \\ \dot{Y} \end{pmatrix} - \frac{1}{2}\begin{pmatrix} -C_2 & C_3 \\ -C_3 & -C_2 \end{pmatrix}\begin{pmatrix} X \\ Y \end{pmatrix} \tag{6}$$

In formula (6), *X* and *Y* are dimensionless displacements at the axis diameter, $\dot{X}$ and $\dot{Y}$ are dimensionless velocities. Namely, $X=x/\delta$, $Y=y/\delta$, $\dot{X}=\dot{x}/\delta\omega$, $\dot{Y}=\dot{y}/\delta\omega$. Additional parameters are detailed in literature [2].

III. Nonlinear Dynamics Analysis of Oil Film Instability in Double-Span Rotor System

The main parameters of the system are as follows: the axis diameter of rotor system is 10mm, and total length is 820mm. The first span is 500mm, the second span is 320mm, and the two axes are connected by rigid coupling. The first natural frequency of the system is 40Hz. Assuming that the eccentricity acts on the disk, and the unbalance is 120g•mm, without phase difference. The material density of the system ρ=7830kg/m^3 , modulus of elasticity E=2.19×10^{11}Pa , and Poisson's ratio v=0.3 . Sliding bearings are used on the left side of the first span. The oil film force parameters are as follows: bearing diameter L=20mm, bearing width D=40mm, oil film clearance C=300um, lubricant viscosity η=0.04Pa·s . The other bearings are self-lubricating graphite bearings, bearing seat weight 800g, stiffness $k_1=3\times10^8 N/m$ and damping $c_1=5\times10^5 N\cdot s/m$.

Newmark-β numerical integration method is used to calculate the results. For the sake of observing the motion characteristics of the system better, as Figure 2(a) shows, the oil film oscillation occurs when the Initial condition's system speed reaches 7000r/min. The oil hydraulic oscillation frequency increases instantaneously, and amplitude decreases when the power frequency is suppressed, and the oil film oscillation frequency exceed power frequency amplitude. When the speed is within the scope in 7000r/min-10000r/min,

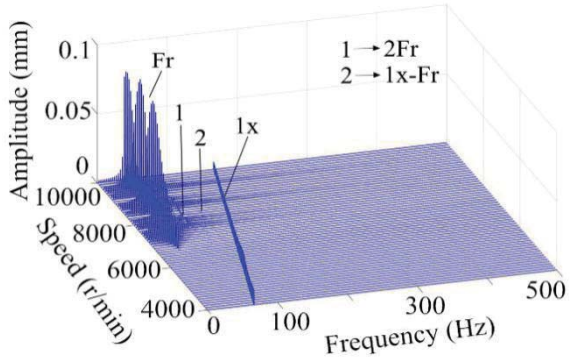

(a) Initial condition

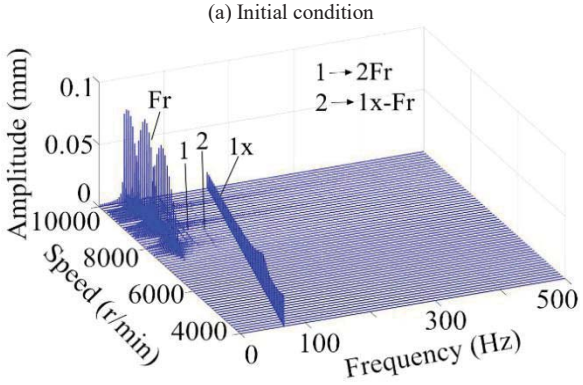

(b) The eccentricity of 280g•mm

Figure 2. 3-D waterfall plot of the start-up of rotor system

the amplitude of oil film oscillation frequency increases and decreases three times, the three peaks are similar, and there are two times of oil film oscillation frequency and other combination frequency components. When the eccentricity is 280g•mm, the 3-D waterfall diagram of the system is shown as Figure 2(b). The motion characteristics of the system are similar to the initial conditions, but the amplitude of the low frequency components produced by the oil film oscillation decreases with the increase of the power frequency amplitude and the delay of the rotation rate of the oil film oscillation.

In order to observe the motion trajectory and characteristics of sliding bearings intuitively, the motion characteristics images with obvious phenomenal characteristics are drawn.

Figure 3(a) is the dynamic characteristics of the system at a speed of 7000r/min. It can be seen that the axis trajectory is

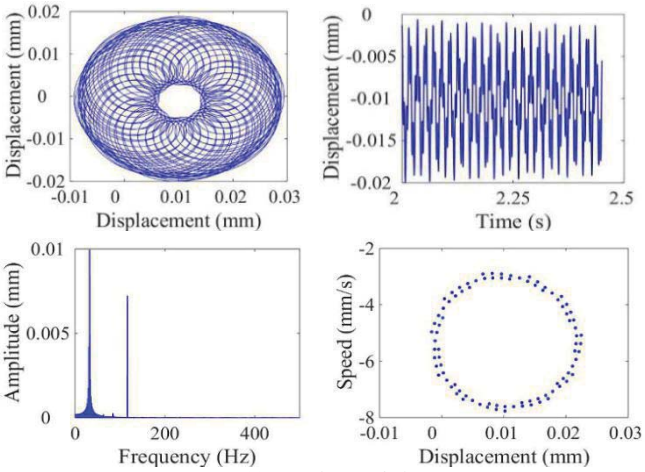

(a) Speed 7000r/min

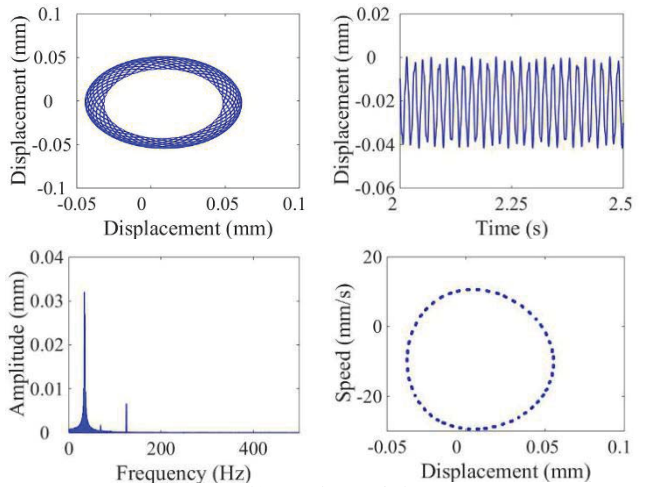

(b) Speed 7500r/min

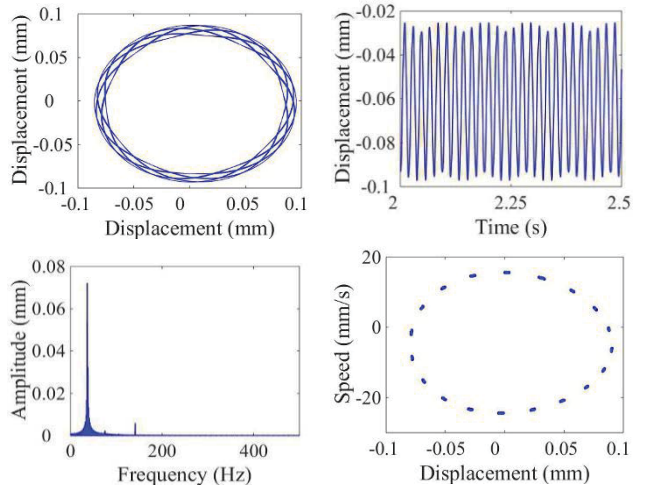

(c) Speed 8500r/min

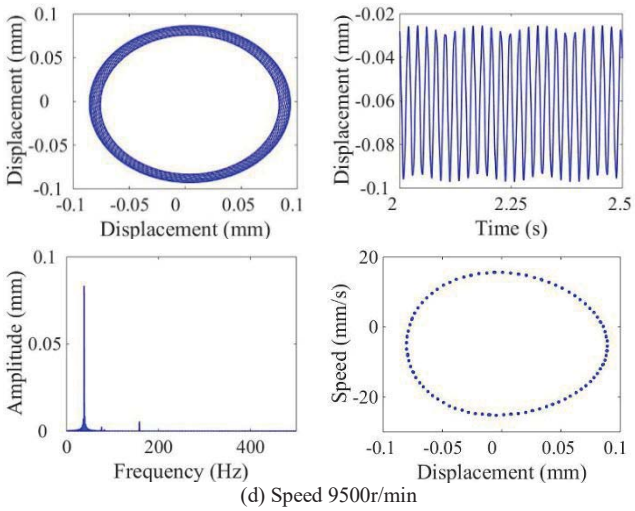

(d) Speed 9500r/min

Figure 3. Axis trajectory, time domain waveform, spectrum and Poincare section of the test point at different rotation rates

surrounded by many inward "8" words in the center, similar to the shape of a flower. The Poincare diagram is a set of point divergent outward. At this time, the oil film oscillation frequency is slightly higher than the power frequency amplitude, when the system is chaotic; Figure 3(b) show the response of the system at a speed of 7500r/min, and the axis trajectory is more. Poincare section diagram demonstrates numerous sets of dots in a circle, so the system makes quasi-periodic motion. As shown in Figure 3(c), when the speed of the system reaches 8500r/min, the trajectory becomes larger and the oil film oscillation frequency reaches the highest. The Poincare section diagram shows that the system makes double periodic motion at this time. The speed of the system shown in Figure 3(d) is 9500r/min. The dynamic characteristic is the same as that at 7500r/min, when the rotation system is in quasi-periodic fettle.

Response diagram under the condition of the system parameter eccentricity varying to 280g•mm is shown in Figure 4. Figure 4 (a) is the system response diagram when the

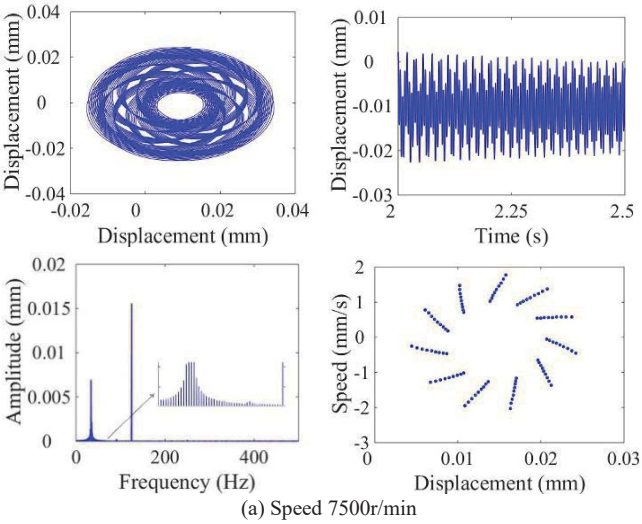

(a) Speed 7500r/min

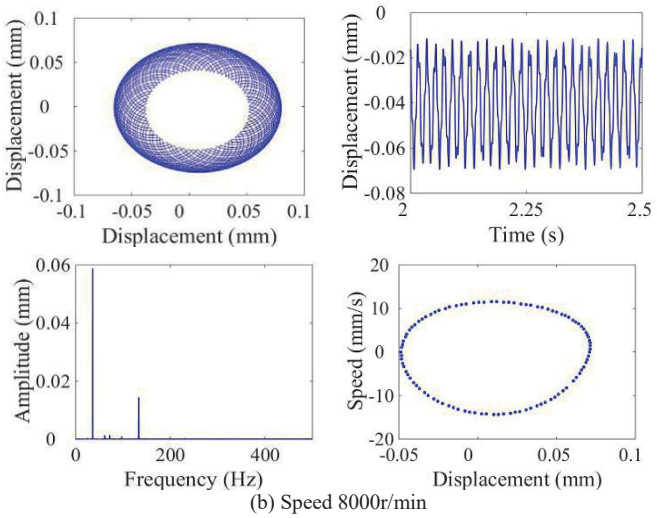

(b) Speed 8000r/min

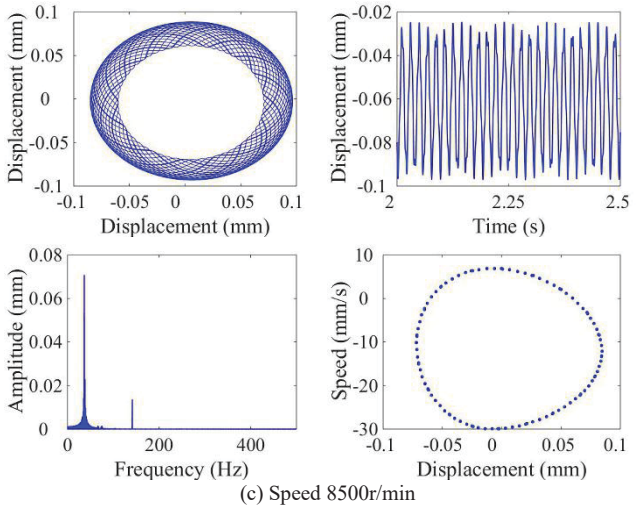

(c) Speed 8500r/min

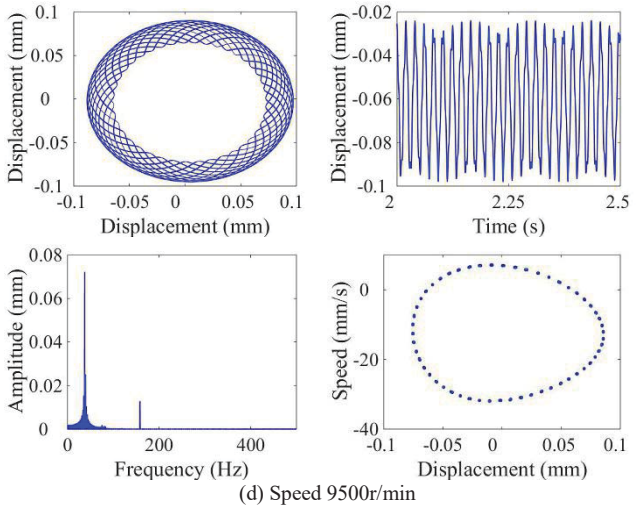

(d) Speed 9500r/min

Figure 4. Axis trajectory, time domain waveform, spectrum and Poincare section of the test place at different speeds

speed is 7500r/min. Its axis trajectory is dense large circles with small circles. FFT shows that the oil film oscillation frequency is slightly lower than the power frequency. Poincare cross-section is a point set divergent around the circumference. At this time, the system makes chaotic motion. When the speed reaches 8000r/min as revealed in Figure 4(b), the axis trajectory of the test place is a ring network composed of several groups of curves. FFT can see that the low frequency amplitude has exceeded the power frequency amplitude, Poincare diagram is a closed point set around a circle, and the rotation makes quasi-periodic fettle at this time. The system response diagram of 8500 r/min and 9500 r/min is shown in Figure 4 (c) and 4 (d). The axis trajectory of the system motion is similar to that of 4 (b). FFT can see that the amplitude of oil film oscillation frequency is lower than the initial condition at this speed, and the power frequency amplitude increases. The Poincare cross section shows that the system continues to do quasi-periodic motion.

IV. Experiments on Double-Span Rotor-Sliding Bearing System

A. Introduction of Laboratory Platform

The structure of the double-span rotor experimental device is shown in Figure 5. The experimental platform is composed of V-type base, base bracket, speed regulating motor, sensor and bearing base, flexible coupling, oil film shaft, rotating disc and motor governor. The dual-span dual-rotor system is composed of a long, a short, two rotating shafts and two discs, connected by a rigid coupling in the middle and supported by three self-lubricating graphite bearings and one sliding bearing. The motor is fixed on the base and connected with the flexible coupling through the rotating shaft, which drives the rotor system to rotate and cooperates with the controller to realize the speed regulation function. There are two types of sensors installed in the system. One is photoelectric sensor, which is used to measure the rate of the test place. The other are displacement sensors, which is used to survey the vibration and orbit of the axis by installing the horizontal and vertical positions of the two rotating axes respectively.

Figure 5. Schematic diagram of a double span rotor platform

B. Analysis of experimental results

The test is a qualitative analysis. According to Figure 6(a), first order critical speed of the two-span system is 2100 r/min. Because of the limitation of the test-bed, the speed of the rotor test-bed can't be raised to the second critical speed or above. Therefore, the response of the system at the rotational rate of 1000-7700 r/min is studied only. By adjusting the motor governor, the oil liquid instability of test place is selected and axis trajectory and frequency spectrum are observed. By adding 1.6g eccentric mass to the disc near the sliding bearing, the three-dimensional waterfall diagram of the system's speed-up process and the stable speed response diagram of the test point at steady speed are recorded again, and the dynamic characteristics of the two cases are compared and analyzed.

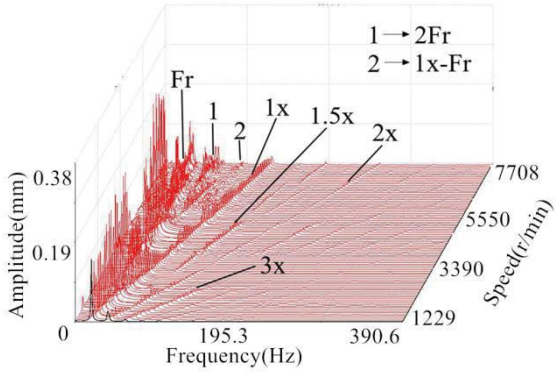

(a) No eccentricity

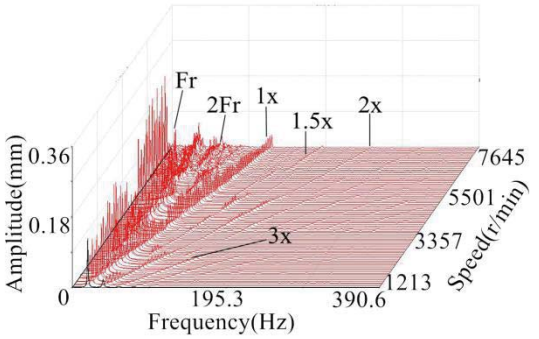

(b) The case of eccentricity 1.6g

Figure 6. 3-D waterfall plot of the start-up of rotor system

The three-dimensional waterfall diagram of acceleration without eccentric mass is revealed in Figure 6(a). It can be found out from the figure when the rate is less than 3500r/min, the system shows positive synchronization. Besides the power frequency, there are also high frequency components with smaller peaks, such as 2-fold and 3-fold. Oil film whirl occurs at the rotor velocity in 3500 r/min-4300 r/min, the half-frequency component increases gradually, and the power frequency amplitude is suppressed and decreased continuously. The oil whirl disappears when the velocity is in 4300 r/min-4700 r/min, which is restrained by the increase of power frequency. In the rate range of 4900r/min-7700r/min, the phenomenon of "frequency locking" occurs in the system. At this time, oil liquid oscillation occurs in the rotator system. The low frequency amplitude of oil film oscillation undergoes three times of rise and fall and is always higher than the power frequency. The peak value reaches near 5750r/min, and other frequency doubling components gradually appear.

When the eccentric mass is 1.6g, the three-dimensional waterfall diagram of the test point is revealed in Figure 6(b). Compared with the case without eccentricity, the power frequency amplitude of the system at the first critical speed decreases. Oil film whirl occurs at the system speed of 2900 r/min-3800 r/min. Oil film oscillation occurs in the velocity range of 4500 r/min-7700 r/min, and the low frequency amplitude of oil film oscillation decreases suddenly when the rate is 6400 r/min. This may be owing to the increase of eccentric mass and the suppression of oil oscillation. The power frequency amplitude is higher than that without eccentricity, and the oil liquid oscillation frequency and other low frequency components are decreasing.

The axle center trajectory and FFT of the test place in the case of oil whirl and oil fluid oscillation are analyzed in detail. As depicted in Figure 7. From Figure 7(a), it can be observed when the rotational rate of the motor is 3500 r/min, the half-frequency is slightly lower than the power frequency, and the axis trajectory is superimposed by multiple ellipses. At this time, the rotor moves in multiple periods. From Figure 7(b), it can be seen that when the rotating speed is 6000r/min, the axis trajectory is composed of several complex and confused curves.

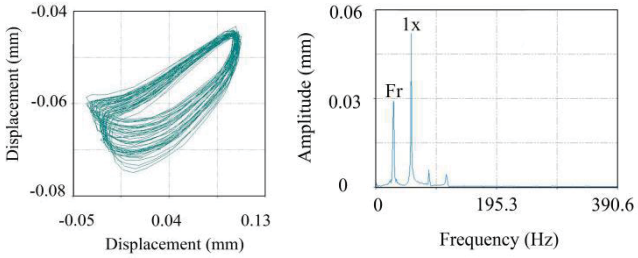

(a) Speed 3500r/min

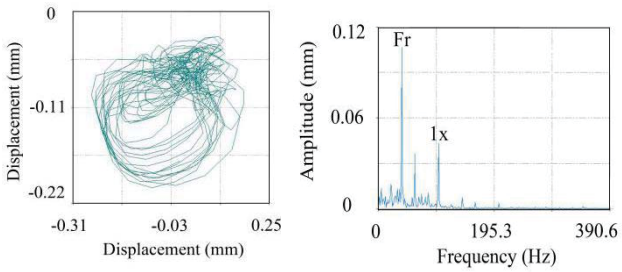

(b) Speed 6000r/min

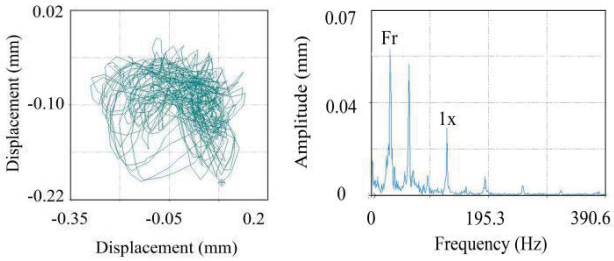

(c) Speed 7500r/min

Figure 7. Axis track and spectrum of rotor system at different rotational speed without eccentricity

There are many low-frequency components in the spectrum and a combination frequency. At this time, oil oscillation occurs in the rotor. As shown in Figure 7(c), when the rotator rate reaches 7500r/min, it can be seen from the spectrum that besides the frequency of conversion and oil film oscillation, there is also a 3/2 oil film force frequency component with a higher amplitude. The axis trajectory of the rotor is still a chaotic and complex curve, and the system is continuously in oil fluid oscillation.

The response of the rotator with increasing eccentricity is shown in Figure 8. As shown in Figure 8(a), when the motor speed is 2950r/min, the axis trajectory is an inner "8" shape, which is the dynamic characteristic of typical oil film whirl. When the rate of the motor is 6000r/min, as is shown in Figure

8(b). There is two times the oil film oscillation frequency appearing. The axis trajectory is three circles. At this time, the system moves in period 3, and its motion characteristics are completely different from those without deviation. From figure 8(c), it can be observed that when the motor speed is 7500r/min, the axis trajectory is a lot of complex and irregular curves. FFT contains many continuous sum and difference combination frequencies, but the amplitude of its low frequency component is lower than that of the non-eccentric condition. At this time, oil film oscillation occurs continuously in the system.

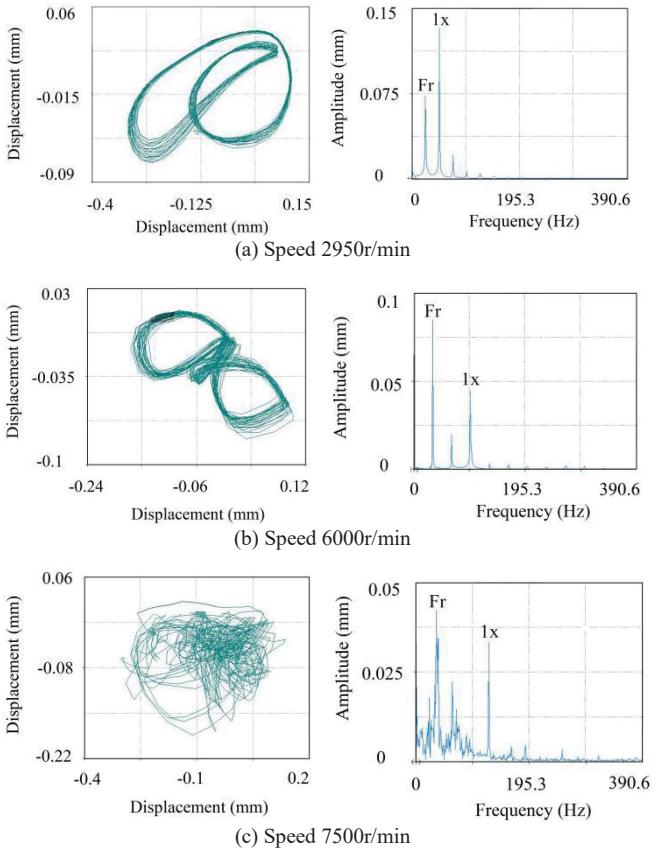

Figure 8. Axis center track and spectrum of rotor system with eccentric mass of 1.6g at different rotational speed time domain waveform diagram at critical speed range

V. CONCLUSION

Numerical simulation and experimental measurements are carried out for oil liquid instability faults of a two-span rotator-bearing system. The results show that:

(1). Results of numerical simulation are given. With the eccentricity is properly increased in the dual-span rotor-bearing system, the amplitude of the frequency which is produced by oil film oscillation decreases. The power frequency amplitude increases and the displacement of the system trajectory increases after the speed reaches 7500 r/min. It shows that increasing eccentricity properly can restrain the effect of oil film instability, but also increase the instability of system operation.

(2). Experiments show that the oil film whirl and oil film oscillation occur in turn during the operation of the system from low speed to high speed. When the oil film whirls, the half-frequency component appears in the system and half-frequency amplitude is small. After 2 times of the first critical speed, the oil film oscillation occurs, the half-frequency amplitude peaks and the axis trajectory is in disorder. Oil film instability can trigger the combination frequency of power frequency and instability frequency besides low frequency, in which the low frequency component incited by oil liquid instability is leading position. The amplitude of low frequency components produced by oil film oscillation decreases with addition of eccentricity. It indicates that oil film oscillation can be restrained to a certain extent. Both numerical simulation and experimental results can confirm this rule.

ACKNOWLEDGMENT

The project supported by the Major Program of the Nationa l Natural Science Foundation of China (Grant No.51875085), a nd the Natural Science Foundation of Liaoning Province, China (Grant No. 20170540205, 20180551073).

REFERENCES

[1] G. Capone, Analytical description of fluid-dynamic force field in cylindrical journal bearing. L'Energia Elettrica 3 (1991) 105–110.

[2] Zhang W, et al. Modeling of nonlinear oil-film force acting on a journal with unsteady motion and nonlinear instability analysis under the model. International Journal of Nonlinear Sciences and Numerical Simulation, 2000, 1(3) 179–186.

[3] Xiang L, Hu A.J, Hou L.L, & Xiong Y.P. Nonlinear coupled dynamics of an asymmetric double-disc rotor-bearing system under rub-impact and oil-film forces. Applied Mathematical Modelling, 40 (2016) 4505–4523

[4] J.P. Jing, G. Meng, Y. Sun, S.B. Xia, On the non-linear dynamic of a rotor-bearing system, Journal of Sound and Vibration, 274 (2004) 1031–1044.

[5] J.P. Jing, G. Meng, Y. Sun, S.B. Xia, On the whipping of a rotor-bearing system by a continuum model, Applied Mathematical Modelling 29 (2005) 461–475.

[6] Ma, H, Li, H, Zhao, X, Niu, H.Q, & Wen, B.C. (2013). Effects of eccentric phase difference between two discs on oil-film instability in a rotor–bearing system. *Mechanical Systems and Signal Processing, 41*(1-2), 526-5450.

[7] Ma H., Li H, Niu H. , Song R. , & Wen, B.C. Nonlinear coupled dynamics of an asymmetric double-disc rotor-bearing system under rub-impact and oil-film forces[J]. Journal of Sound and Vibration 332 (2013) 6128–6154.

[8] Ma H, Li H, Zhang S.Y, & Wen, B.C. Simulation and experiment research on the second order oil-film instability fault in a rotor system. Journal of Mechanical Engineering, 2013, 49(9):24.

[9] Han Q.K., Ren Y.P., Liu K., & Wen B.C. Experimental Analysis on Vibration of Rotor System with Oil-Film Instability Fault [J]. Journal of Northeastern University (Natural Science), 2003(10):959-961.

[10] Liu X.F. , Luo H.L. , Luo Y.L. Method for analysis of instable journal bearing signal based directional adaptive optimal kernel distribution [J]. Journal of Vibration and Shock, 2016, 35(10):151-156.